

**Predicting East  
African spring  
droughts**

C. Funk et al.

This discussion paper is/has been under review for the journal Hydrology and Earth System Sciences (HESS). Please refer to the corresponding final paper in HESS if available.

# Predicting East African spring droughts using Pacific and Indian Ocean sea surface temperature indices

C. Funk<sup>1,2</sup>, A. Hoell<sup>2</sup>, S. Shukla<sup>2</sup>, I. Bladé<sup>3</sup>, B. Liebmann<sup>4</sup>, J. B. Roberts<sup>5</sup>,  
F. R. Robertson<sup>5</sup>, and G. Husak<sup>2</sup>

<sup>1</sup>US Geological Survey, Santa Barbara, USA

<sup>2</sup>University of California Santa Barbara Geography, Santa Barbara, USA

<sup>3</sup>Institut Catala de Ciències del Clima, Departament d'Astronomia i Meteorologia, Facultat de Física, Universitat de Barcelona, Barcelona, Spain

<sup>4</sup>NOAA Earth Systems Research Laboratory, Boulder, CO, USA

<sup>5</sup>NASA Marshall Space Flight Center, Huntsville, LA, USA

Received: 21 February 2014 – Accepted: 3 March 2014 – Published: 20 March 2014

Correspondence to: C. Funk (cfunk@usgs.gov)

Published by Copernicus Publications on behalf of the European Geosciences Union.

Title Page

Abstract

Introduction

Conclusions

References

Tables

Figures

⏪

⏩

◀

▶

Back

Close

Full Screen / Esc

Printer-friendly Version

Interactive Discussion



## Abstract

In southern Ethiopia, Eastern Kenya, and southern Somalia, poor boreal spring rains in 1999, 2000, 2004, 2007, 2008, 2009, and 2011 contributed to severe food insecurity and high levels of malnutrition. Predicting rainfall deficits in this region on seasonal and decadal time frames can help decision makers implement disaster risk reduction measures while guiding climate-smart adaptation and agricultural development. Building on recent research that links more frequent droughts in that region to a stronger Walker Circulation, warming in the Indo-Pacific warm pool, and an increased western Pacific sea surface temperature (SST) gradient, we show that the two dominant modes of East African boreal spring rainfall variability are tied, respectively, to western-central Pacific and central Indian Ocean SST. Variations in these rainfall modes can be predicted using two previously defined SST indices – the West Pacific Gradient (WPG) and Central Indian Ocean index (CIO), with the WPG and CIO being used, respectively, to predict the first and second rainfall modes. These simple indices can be used in concert with more sophisticated coupled modeling systems and land surface data assimilations to help inform early warning and guide climate outlooks.

## 1 Introduction

Since 2003, scientists from the University of California, Santa Barbara's Climate Hazards Group, the US Geological Survey, the National Ocean and Atmospheric Administration's (NOAA) Earth System Research Laboratory, Physical Science Division, Climate Analysis Branch, and the National Aeronautics and Space Agency have been working to improve the US Agency for International Development's Famine Early Warning System Network's (FEWS NET) drought early warning capabilities for Eastern Africa. Early efforts focused on developing better Ethiopian rainfall archives and historical time series and revealed substantial 1980–2004 rainfall declines in key crop growing areas in the southern half of the country. Further diagnostic analysis (Verdin

**HESSD**

11, 3111–3136, 2014

## Predicting East African spring droughts

C. Funk et al.

Title Page

Abstract

Introduction

Conclusions

References

Tables

Figures

◀

▶

◀

▶

Back

Close

Full Screen / Esc

Printer-friendly Version

Interactive Discussion



**Predicting East African spring droughts**

C. Funk et al.

[Title Page](#)[Abstract](#)[Introduction](#)[Conclusions](#)[References](#)[Tables](#)[Figures](#)[⏪](#)[⏩](#)[◀](#)[▶](#)[Back](#)[Close](#)[Full Screen / Esc](#)[Printer-friendly Version](#)[Interactive Discussion](#)

et al., 2005) of sea surface temperatures (SST) and precipitation suggested that the emergence of more very warm ( $> 29^{\circ}\text{C}$ ) areas in the south-central Indian Ocean and equatorial western Pacific was tied to an increase in local precipitation over the ocean and reduced rainfall over Eastern Africa through a Rossby wave-like (Gill, 1980) atmospheric response. Further analysis (Funk et al., 2008) examined the canonical correlation between moisture transports over Eastern Africa and reanalysis precipitation over the Indian Ocean. Increased precipitation over the south Central Indian Ocean (CIO,  $0\text{--}15^{\circ}\text{S}$ ,  $60\text{--}90^{\circ}\text{E}$ ) was found to be associated with decreased easterly moisture flows into the Horn of Africa. Further confirmation of this relationship was obtained from an experiment using on the Community Atmospheric Model (CAM), suggested that anomalous diabatic heating over the Indian Ocean reduced and disrupted onshore moisture transports.

These diagnostic analyses were extended by using a joint Principal Component Analysis (PCA) based zonal surface winds, 500 hPa vertical velocities, rainfall and SSTs over the tropical Indo-Pacific Area (IPA) (Williams and Funk, 2011). The leading principal component (PC) was shown to represent a low frequency warming signal associated with an enhancement of the Walker circulation over the western Pacific and Indian Ocean, and declining rainfall across Eastern Africa and the central equatorial Pacific. Specifically, Figs. 7 and 8 of Williams and Funk identified low level convergence over the warm pool and increases in convection, ridging over the eastern Horn, westerly near surface zonal wind anomalies over the northern equatorial Indian Ocean, and reductions in total atmospheric precipitable water.

The 2nd PC was well correlated with Niño 4 SSTs ( $5^{\circ}\text{S}\text{--}5^{\circ}\text{N}$ ,  $160^{\circ}\text{E}\text{--}150^{\circ}\text{W}$ ). The spatial pattern associated with this component identified concomitant warming and precipitation increases across the central Indian *and* western Pacific oceans. Both the 1st and 2nd PCs were found to be associated with zonally overturning circulation anomalies and subsidence over Eastern Africa. The spatial and temporal structure of these circulations varied; while the 1st PC varied on low frequency time scales and had a

pattern concentrated over the warm pool, the 2nd PC tracked with El Niño-Southern Oscillation (ENSO) variations.

The IPA PC1, which was linked to warming warm pool Indo-Pacific SST, was associated with East African drought in two ways. First, correlations between PC1 and reanalysis data showed that increased PC1 values were associated with dry subsiding air over the Horn, reduced onshore moisture transports and terrestrial precipitation declines. These relationships helped explain the downward 1980–2009 rainfall trends across the eastern portions of the Greater Horn of Africa. Second, it was hypothesized that the subsidence produced by increases in PC1 might combine with the effects of La Niña to create stronger East African drought teleconnections. Both the IPA PC1 and ENSO are associated with increased vertical velocities over the equatorial Indo-Pacific, and increased subsidence and higher surface pressures over East Africa. To test whether these influences might combine, 1950–2009 La Niña events were categorized into positive and negative PC1 categories and composited. Composites of positive PC1 La Niña events identified a much stronger negative response over Eastern Africa during “new” high 1st PC La Niña events (Williams and Funk, 2010). Over our study region, composites of low PC1 La Niña events had standardized precipitation index (SPI) (McKee et al., 1993) values of about  $-0.1$ , while composites of high PC1 La Niña events had SPI values ranging from  $-0.4$  to  $-0.8$ . In the summer of 2010, when our NOAA partners predicted that there was a high probability for the development of a strong La Niña, FEWS NET used composites of high IPA PC1 La Niña seasons to provide early warning of the devastating 2011 drought (Ververs, 2011).

In 2012, new research (Lyon and DeWitt, 2012) suggested that a 1999–2011 shift in Pacific SSTs had played an important role in increasing the intensity of the Walker circulation, drying eastern Africa. In that study several sets of atmospheric general circulation model simulations were run to isolate the Indian and Pacific effects. Indian Ocean forcing produced anomalous circulations similar to those identified in prior FEWS NET analyses of Indian Ocean influences (Funk et al., 2005, 2008; Jury and Funk, 2013; Verdin et al., 2005; Williams et al., 2011). The Pacific Ocean forcing effects

## HESSD

11, 3111–3136, 2014

### Predicting East African spring droughts

C. Funk et al.

Title Page

Abstract

Introduction

Conclusions

References

Tables

Figures

⏪

⏩

◀

▶

Back

Close

Full Screen / Esc

Printer-friendly Version

Interactive Discussion



were consistent with those detected in the IPA analysis of Williams and Funk (2011). In a more recent study, Lyon et al. (2013) have focused primarily on the role of internal Pacific Decadal Variability on generating a potential climate shift around 1998. Other studies (Funk, 2012; Williams and Funk, 2011) have instead highlighted the similarity between recent observed western Pacific and Indian Ocean SST changes and the predicted warming in climate change models. Of course the real answer may involve a combination of natural and anthropogenic causes. Analyses of simulations with the Global Forecast System model, driven with observed SST (Funk et al., 2013; Hoell and Funk, 2013b), and similar simulations with the ECHAM5 model (Liebmann et al., 2013), speculate that both low frequency warming in the western Pacific and natural inter-annual and decadal Pacific SST variations can account for some of East Africa's drying trend.

While debate seems likely to continue regarding the origin of the SST signals responsible for recent East Africa droughts, long rain declines have been confirmed by many studies (Funk et al., 2012; Hoell and Funk, 2013a, b; Liebmann et al., 2013; Lyon et al., 2013; Viste et al., 2012). As our understanding of the causes of recent droughts increases, so do our opportunities for effective predictions. While prior studies, based on 1958–1997 data, indicated a weak zonal circulation over the equatorial ocean, and a related weak correlation between East African rainfall and zonal winds over the Indian Ocean (Hastenrath et al., 2011), more recent analyses of 1993–2012 GFS precipitation simulations (Funk et al., 2013) and CMAP precipitation (Lyon and DeWitt, 2012) suggest that over the past twenty years dry East African seasons were associated with a precipitation dipole over the western and central Pacific. Vigorous western Pacific precipitation increase the chance of dry East African long rains (Liebmann et al., 2013), and the co-occurrence of La Niña events with a strong WPG events leads to anomalous western Pacific precipitation increases (Hoell and Funk, 2013a). The WPG is defined as the difference between SST in the Niño 4 region (160° E–150° W, 5° S–5° N) and the western Pacific (WP, 130–150° E, 0–20° N). The combination of strong WPG and La Niña events produces large SST gradients across the entire equatorial Pacific and

## Predicting East African spring droughts

C. Funk et al.

[Title Page](#)[Abstract](#)[Introduction](#)[Conclusions](#)[References](#)[Tables](#)[Figures](#)[⏪](#)[⏩](#)[◀](#)[▶](#)[Back](#)[Close](#)[Full Screen / Esc](#)[Printer-friendly Version](#)[Interactive Discussion](#)

this appears to be conducive to vigorous WP precipitation and increased subsidence across the Horn of Africa. WP SST (Hoell and Funk, 2013b) and the WPG (Hoell and Funk, 2013a) have increased dramatically over the past thirty years, increasing the frequency of co-occurring WPG/La Niña events, and we hypothesize, creating opportunities for drought prediction.

The purpose of this paper is to demonstrate how indices based on our prior research (WPG and CIO) can be effectively used to monitor and predict East African boreal spring (March–May) rainfall. The PC and regression based analyses presented here can help overcome some of the limitations of coupled ocean–atmosphere models, which have difficulty recreating East African rainfall variations (Mwangi et al., 2014). The WPG and CIO indices can link the process-based studies discussed above with the needs of real time monitoring and climate diagnostics. Such analysis has helped FEWS NET identify analog years and effectively communicate risks to decision makers in 2011 (Ververs, 2011) and 2012 (US, 2012). There are important climate indices, beyond the well-known measures like Niño 3.4 SSTs and the Indian Ocean Dipole (IOD) (Saji et al., 1999), that can inform East African climate outlooks, such as the Greater Horn of Africa Climate Outlook Fora. While these indices are good indicators for the region’s boreal fall “short” rains, the WPG and CIO may be preferable during boreal spring.

The prediction targets examined here are the first and second principal components (PC1 and PC2) of precipitation for the 1981–2013 time period, estimated using the new  $0.05^\circ \times 0.05^\circ$  gridded Climate Hazards group Infrared Precipitation with Stations (CHIRPS) data (Funk et al., 2014). We briefly describe the CHIRPS; then we explore the pattern and time series associated with the first two principal components during the March–May season. Spatial correlations between these principal components and antecedent (January) SST show that PC1 corresponds to Pacific SST gradients similar to the WPG, and supported by more recent analyses (the 2011–2013 citations discussed above). The PC2 SST correlation structure, on the other hand, is similar to earlier (2005–2008) research focused on the CIO. The boreal spring long rains

# HESSD

11, 3111–3136, 2014

## Predicting East African spring droughts

C. Funk et al.

[Title Page](#)

[Abstract](#)

[Introduction](#)

[Conclusions](#)

[References](#)

[Tables](#)

[Figures](#)

[⏪](#)

[⏩](#)

[◀](#)

[▶](#)

[Back](#)

[Close](#)

[Full Screen / Esc](#)

[Printer-friendly Version](#)

[Interactive Discussion](#)



teleconnections for East Africa are very different from the boreal fall short rains (Hoell and Funk, 2013b; Liebmann et al., 2013); while the short rains are well correlated to SST in the far western Indian Ocean and far eastern Pacific, the long rains exhibit a stronger relationship to WPG and CIO SST. Here, we show that the WPG and CIO indices can be useful large scale climate indicators by using them to predict the 1st and 2nd principal components (PC1 and PC2) of the CHIRPS March–May East African rainfall. We relate PC1 to the WPG, and PC2 to CIO SST. We then show that these simple indices provide a reasonable basis for forecasting some East Africa extremes. The paper concludes with a brief analysis of long term changes in WPG SSTs in both observations and model simulations.

## 2 Data

This study focuses mainly on the relationships between CHIRPS March–May rainfall over a region extending across the southern Arabian peninsula and eastern East Africa (25–55° E, 13° S–20° N) and January NOAA Extended Reconstruction version 3b SST (ER3b) (Smith et al., 2008). The CHIRPS study precipitation region was selected based on (i) the climatological importance of March–May rainfall, (ii) a known sensitivity to Indo-Pacific forcing and (iii) high underlying levels of food and water insecurity. The study focuses on Yemen, Djibouti, Eritrea, Ethiopia, Somalia, Kenya, and Tanzania.

The 1981–2013 CHIRPS data set (Funk et al., 2014) combines satellite cold cloud duration rainfall estimates with gauge observations and a high resolution (0.05°) precipitation climatology. Comparisons between the CHIRPS fields and two state-of-the-science data sets: the Global Precipitation Climatology Centre data set (Schneider et al., 2013), and the Global Precipitation Climatology Project (Adler et al., 2003) data sets, reveal a reasonable level of correspondence among all three data sources. We compare the major modes of variability (principal components) of the March–May CHIRPS with January SSTs from the Extended Reconstruction version 3b SST (ER3b) (Smith et al., 2008).

**HESSD**

11, 3111–3136, 2014

### Predicting East African spring droughts

C. Funk et al.

[Title Page](#)

[Abstract](#)

[Introduction](#)

[Conclusions](#)

[References](#)

[Tables](#)

[Figures](#)

[⏪](#)

[⏩](#)

[◀](#)

[▶](#)

[Back](#)

[Close](#)

[Full Screen / Esc](#)

[Printer-friendly Version](#)

[Interactive Discussion](#)





in mid-February at the Greater Horn of Africa Climate Outlook Forum (GHACOF) to produce a regional forecast for East Africa.

Figure 1 shows the first and second principal component maps and time series for our extended East African region. The principal components were calculated based on the 1981–2013 covariance matrix. PC1 and PC2 explained 26 and 12 %, respectively, of the total rainfall variance in the study region. Figure 1a and b show the changes in standardized precipitation associated with PC1 and PC2. The principal component spatial patterns have been scaled by the 1981–2013 trends in PC1 and PC2, and then divided by the standard deviation of rainfall at each location. This provides an estimate of the 20 year change in the standardized precipitation associated with the first and second mode. This can help us understand the contributions of changes in the first and second principal components to the observed trends (Fig. 2c).

Figure 1a indicates substantial rainfall declines extending from northern Tanzania through Yemen, with the strongest standardized declines occurring just north of the equator. The precipitation declines associated with this mode have been large (often more than half a standard deviation). Figure 1b was created in an identical fashion, using PC2. This pattern tends to emphasize off-equatorial regions of Tanzania, northern Ethiopia, Eritrea, and Djibouti. Figure 1d shows the time series for these principal components. The first principal component identifies many large drought years: 1984, 1992, 1999, 2000, 2004, 2008, 2009, and 2011. The large negative PC2 values in 1988, 2003, 2008, 2009, and 2013 were associated with dryness in Tanzania and Ethiopia, but not near the equator. Both time series exhibit substantial interannual variations and substantial declines between the 1980s 1990s and 21st century.

The total rainfall trend for this period is presented in Fig. 1c. This trend pattern suggests that the substantial rainfall declines that have occurred during the last 20 years can be ascribed, partially, to the two leading modes. We next examine the relationships between these time series and antecedent January SST. January SST were selected as a basis for monitoring and prediction because data from this month can be used to inform analyses carried out by African scientists in early February at the GHACOF.

## HESSD

11, 3111–3136, 2014

### Predicting East African spring droughts

C. Funk et al.

[Title Page](#)

[Abstract](#)

[Introduction](#)

[Conclusions](#)

[References](#)

[Tables](#)

[Figures](#)

[⏪](#)

[⏩](#)

[◀](#)

[▶](#)

[Back](#)

[Close](#)

[Full Screen / Esc](#)

[Printer-friendly Version](#)

[Interactive Discussion](#)



Such analyses can also inform regional food security outlooks, providing sufficient lead time to inform contingency plans, guide resource distribution, and help pre-position humanitarian assistance.

### 3.2 Correlations with January SST

5 The correlation results presented here use a 1994–2013 comparison period because the studies discussed above indicate a recent increase in the sensitivity of East African precipitation to Indo-Pacific SST forcing, and because our ultimate focus is on predicting droughts in an operational setting over the next few years. While our research has suggested that this sensitivity is tied to a long term warming trend, and a stronger Walker circulation (Williams and Funk, 2011) as well as a stronger WPG (Hoell and Funk, 2013b; Hoell et al., 2014), a future transition to a warmer central Pacific might weaken the boreal Spring teleconnection pattern.

15 The correlations (Fig. 2a) between the March–May PC1 (solid red line, Fig. 1d) and the preceding January SST field indicate that a stronger than normal west-to-east Pacific SST gradient over the tropical Pacific is associated with dry conditions over most of the Horn of Africa, consistent with earlier findings (Tierney et al., 2013; Lyon and DeWitt, 2012; Liebmann et al., 2013; Hoell et al., 2013; Hoell and Funk, 2013a, b, c; Funk et al., 2013). The blue and red boxes denote the Niño 4 and WP regions; the WPG index is estimated as the difference between these regions following Hoell and Funk (2013b).

25 The correlation pattern associated with PC2 (Fig. 2b) identifies warming in the Indian Ocean with drying in parts of the Horn of Africa, particularly Ethiopia and Tanzania. These results are also consistent with prior research focusing on the causes of Ethiopian rainfall declines, which identified teleconnections to the Indian Ocean (Williams et al., 2011; Funk et al., 2005; Jury, 2010). Thus both warming in the western Pacific and Indian oceans appear to be associated with East African drying.

## Predicting East African spring droughts

C. Funk et al.

Title Page

Abstract

Introduction

Conclusions

References

Tables

Figures

◀

▶

◀

▶

Back

Close

Full Screen / Esc

Printer-friendly Version

Interactive Discussion



### 3.3 Using January WPG and CIO indices to predict March–May CHIRPS PC1 and PC2

Simple climate indices, like the Indian Ocean Dipole (Saji et al., 1999) or NINO3.4 SSTs can support famine early warning activities and the identification of analog years.

5 Those indices, however, appear much better suited to monitoring East Africa’s “short” rains during boreal fall, since rainfall in that season exhibits teleconnections to the western Indian Ocean and eastern Pacific (Liebmann et al., 2013; Hoell and Funk, 2013b). To support hydrologic early warning for the East African long rains, we explore the skill of the WPG and CIO indices.

10 Two regression prediction time periods for the PC1 time series were compared: 1981–2013 and 1994–2013. The PC1 variance explained by the WPG index over the shorter time period was substantially larger, with the WPG index explaining 50% of the PC1 variance as opposed to 12%. Over the more recent time period, the regression slope between the March–May CHIRPS PC1 and the January WPG index indicated a modest negative relationship, with a one standard deviation decrease in the WPG (designating a stronger WP to NINO4 SST gradient) being associated with a 0.5 standardized deviation decrease in PC1. In this study, which focuses on developing a framework to anticipate the next drought, we use the regression coefficients from the shorter time period to estimate rainfall associated with PC1 based on the western Pacific SST gradient index (WPG), while emphasizing the need to monitor the strength of the La Niña-East Africa teleconnection. The strength of this modest teleconnection is quite similar to results obtained from ECHAM5 simulations (Liebmann et al., 2013).

20 For the PC2 time series, we used a regression based on the full period of record (1981–2013), since the negative relationship between SST in the CIO region and PC2 was found to be robust throughout the time period evaluated. The corresponding 1981–2013 regression explained 33% of the total variance of PC2. For every standard deviation increase in CIO SSTs, PC2 declined –0.6 standard deviations.

HESSD

11, 3111–3136, 2014

## Predicting East African spring droughts

C. Funk et al.

Title Page

Abstract

Introduction

Conclusions

References

Tables

Figures

⏪

⏩

◀

▶

Back

Close

Full Screen / Esc

Printer-friendly Version

Interactive Discussion



**Predicting East African spring droughts**

C. Funk et al.

[Title Page](#)[Abstract](#)[Introduction](#)[Conclusions](#)[References](#)[Tables](#)[Figures](#)[⏪](#)[⏩](#)[◀](#)[▶](#)[Back](#)[Close](#)[Full Screen / Esc](#)[Printer-friendly Version](#)[Interactive Discussion](#)

The CHIRPS principal components relate, respectively, to precursor SST anomalies in the Pacific and Indian oceans (Fig. 2). Figure 3a–c shows scatter plots of the 1994–2013 PC1, 1981–1993 PC1 and 1981–2013 PC2 estimates. The y-axes depict the observed March–May principal components from the CHIRPS data (the values are also plotted in Fig. 1d). The x-axes represent regression estimates of these PCs based on either the WPG or CIO indices calculated from January SST). Over the past twenty years, the combination of wintertime La Niña conditions and warm western Pacific SSTs presage low PC1 values (Fig. 3a). Over the 1994–2013 time period, the three most extreme “dry PC1” seasons (1999, 2000 and 2011) are captured well (dark black diamonds). Over the 1981–1993 period, the PC1 WPG relationship was weak (Fig. 3b), consistent with reports of weaker zonal connections to the Indo-Pacific (Hastenrath et al., 2011). The skill of the Indian Ocean index, on the other hand, comes more from distinguishing between high PC2 values associated with relatively cool Indian Ocean SSTs between 1981 and 1996 and low PC2 values related to the warm Indian Ocean conditions that have persisted since 1997. These time periods are denoted respectively, with diamonds and triangles in Fig. 3c.

These simple WPG and CIO indices can thus be used to predict PC1 and PC2, which can then be multiplied against their loading maps and summed to produce hindcasts of East African March–May rainfall. The correlation between these forecasts and observed 1993–2013 CHIRPs rainfall is shown in Fig. 3d. The eastern Horn of Africa, southern Tanzania, Eritrea, Djibouti, and Yemen all exhibit positive correlations. One region of northern Tanzania is modeled poorly, and exhibits negative correlations. This region also exhibits a downward trend, but these declines seem poorly related to WPG/PC1 or CIO/PC2 changes. Regional climate change simulations (Cook and Vizy, 2013) have suggested that this region may be more sensitive to changes in trans-Congo moisture transports, while drying in Kenya, southern Somalia and southern Ethiopia might be related to changes in the Somali Jet.

Figure 4 shows forecast and observed standardized precipitation index maps for a selection of dry and wet seasons. While the index-based forecasts tend to

under-estimate the variance of the rainfall, the ability to discriminate between wet and dry seasons at a regional scale seems promising. While the ability to discriminate between normal and above normal PC1 values seems limited (Fig. 3a), extreme dry years appear to be fairly well predicted. Thus our index-based predictions can capture some of the extreme drought years (2000, 2009, 2011), but do not predict well some above normal wet seasons (such as 2006 and 2013). We hypothesize that there may be a non-linear response to WP and Niño 4 SST variations. Over the past twenty years, during La Niña events, the effects of the long term WP warming trend and ENSO act to reinforce each other, making droughts more predictable. During neutral or positive ENSO phases, East African precipitation may be more influenced by less predictable Indian Ocean SST, variations in the Madden–Julien Oscillation (Pohl and Camberlin, 2006), or internal atmospheric dynamics.

### 3.4 Examining long time series of East African rainfall and SSTs

We briefly examine long time series of East African rainfall and SSTs. Our objective is to place recent East African rainfall declines in a deeper historic context. We limit our analysis to a 1920 start date, due to the small number rain gauge and SST observations prior to that time (Liebmann et al., 2013). We have averaged the GPCP interpolated gauge dataset over our entire study region (25–55° E, 13° S–20° N), converted the resulting time series into a SPI time series (McKee et al., 1993), smoothed the results with ten year running means, and plotted the results in Fig. 5a. Between 1920 and 1980, the GPCP time series exhibits substantial inter-decadal oscillations, indicative of the climate sensitivity of this semi-arid region. After 1980, the GPCP begins a large decline to arrive at a very low decadal average SPI of  $-0.7$ . We have also used a regression based on 1920–2012 January WP and Niño 4 SST data to create standardized estimates of the WPG time series. These estimates, shown in Fig. 5a ( $r = 0.55$ ,  $p = 0.05$ , based on 7 d.f.), fail to recreate the 1920–1980 decadal oscillations, but do capture well the post-1980 GPCP decline. The GPCP peaks during the 1930s and 1980s and declines during the 1950s; these changes do not seem well represented

## Predicting East African spring droughts

C. Funk et al.

[Title Page](#)

[Abstract](#)

[Introduction](#)

[Conclusions](#)

[References](#)

[Tables](#)

[Figures](#)

[⏪](#)

[⏩](#)

[◀](#)

[▶](#)

[Back](#)

[Close](#)

[Full Screen / Esc](#)

[Printer-friendly Version](#)

[Interactive Discussion](#)



by the WPG, and are likely due to non-WPG SST variations, such extra-tropical Pacific Decadal Variations (PDV). Beginning in the mid-1970s, some East Africa drying seems likely to have been associated with warming in the CIO (Funk et al., 2005, 2008). Since about 1990, both a steep increase in WP SST (Hoell and Funk, 2013b) and PDV (Lyon and DeWitt, 2012) have probably contributed to a  $\sim -0.7$  decline in the GPCC SPI time series.

Figure 5b shows the WP and NINO4 time series contributions to the regression estimates shown in Fig. 5a. Only the WP shows a large trend in recent years. These results indicate that warming in the WP, as opposed to cooling in the Niño 4 region, appears to have been the primary driver of recent GPCC declines. This hypothesis is consistent with Atmospheric General Circulation Model (AGCM) analyses suggesting that the trend component of WP SST has been a large driver of East African decadal rainfall variability and drying (Hoell and Funk, 2013b). Additionally, while Niño 4 SSTs have decreased a little over the past twenty years, they have increased since the 1920s, potentially indicating a moistening effect in the Horn. Since the long rains have declined since the 1920s, it seems likely that this decline may be attributed, at least in part, to warming in the WP.

We next examine the relationship between WP SST and the effects of radiative forcing, as represented by a CMIP5 ensemble. Figure 5c shows the smoothed observed WP SST time series and the multi-model ensemble mean WP SST time series from the CMIP5 models listed in Table 1. The smoothed time series track closely ( $r = 0.89$ ,  $p = 0.01$ , based on 7 d.f.). Note that there are “decadal” variations in the radiatively forced CMIP5 SSTs. These fluctuations are caused by the warming impacts of greenhouse gasses, changes in solar insolation, and the cooling effects of aerosols and volcanic eruptions. The CMIP5 WP SST increases in 1930s and 1940s, stabilizes in the 1950s, cools for a brief period in the 1960s, and increases at an accelerated rate since about 1980. These decadal fluctuations match reasonably well with changes seen in the observed SST, except for an observed SST increase in the early 1950s.

## HESSD

11, 3111–3136, 2014

### Predicting East African spring droughts

C. Funk et al.

Title Page

Abstract

Introduction

Conclusions

References

Tables

Figures

⏪

⏩

◀

▶

Back

Close

Full Screen / Esc

Printer-friendly Version

Interactive Discussion



## Predicting East African spring droughts

C. Funk et al.

Title Page

Abstract

Introduction

Conclusions

References

Tables

Figures

◀

▶

◀

▶

Back

Close

Full Screen / Esc

Printer-friendly Version

Interactive Discussion



It is important to realize that these influences can produce low frequency fluctuations that appear similar to natural “internal” decadal variations. An example of this is shown in Fig. 5d. Linear fits to the observed and CMIP5 WP SST time series have been removed and the residuals plotted. Because we have averaged across a large number of CMIP simulations (43), any “internal” variations associated with natural climate variability should be greatly diminished in the CMIP ensemble mean time series. Nonetheless, we see large swings in CMIP WP SST that are caused by changes in radiative forcing. Overall, the residuals from a linear fit to the radiatively forced CMIP5 WP ensemble SST (dashed blue line) correspond closely ( $r = 0.69$ ,  $p = 0.04$ , based on 7 d.f.) with the residuals from a linear fit with to the observed data (solid red line). Much of the decadal and longer variation around a linear fit to the WP SST data is likely due to external radiative forcing, especially over the past thirty years. New research has highlighted the important climate impacts associated with the 1st principal component of detrended SST (Lyon et al., 2013); Fig. 5d suggests that these detrended SST are likely to have decadal variations influenced by changes in greenhouse gasses, aerosols and insolation.

## 4 Summary

Building on recent diagnostic studies, this paper has explored the utility of two simple SST indices related to the first two principal components of East African spring rainfall. Interestingly, the two principal component modes were found to relate to the WPG and CIO, as identified in prior FEWS NET research. Warming in the WP and cooling in the Niño 4 region was related to rainfall deficits across much of the eastern Horn of Africa (lower PC1 values). Warming in the CIO was related to declines in Tanzania and the northeastern Horn (lower PC2 values). Thus warming in both the western Pacific and Indian Ocean has likely contributed to declines in PC1 and PC2. These SST changes, occurring since the mid-1980s, may be attributable to an increase in anthropogenic forcing (Fig. 5).



Shukla et al., 2014) hold forth exciting new prospects for better early warning. If future ocean conditions continue to provide conditions conducive to East African drought, these and future advances may help us be better prepared.

*Acknowledgements.* This research was supported by the USAID Famine Early Warning Systems Network (FEWS NET), NASA SERVIR and NOAA Technical Transitions grant NA11OAR4310151. We would like to thank Libby White for her thoughtful comments.

## References

- Adler, R. F., Huffman, G. J., Chang, A., Ferraro, R., Xie, P., Janowiak, J., Rudolf, B., Schneider, U., Curtis, S., Bolvin, D., Gruber, A., Susskind, J., and Arkin, P.: The version 2 Global Precipitation Climatology Project (GPCP) monthly precipitation analysis (1979–present), *J. Hydrometeorol.*, 4, 1147–1167, 2003.
- Cook, K. H. and Vizi, E. K.: Projected changes in East African rainy seasons, *J. Climate*, 26, 5931–5948, doi:10.1175/JCLI-D-12-00455.1, 2013.
- Funk, C., Senay, G., Asfaw, A., Verdin, J., Rowland, J., Michaelson, J., Eilerts, G., Korecha, D., and Choularton, R.: Recent Drought Tendencies in Ethiopia and Equatorial-Subtropical Eastern Africa, US Agency for International Development, Washington, D.C., 2005.
- Funk, C., Dettinger, M. D., Michaelsen, J. C., Verdin, J. P., Brown, M. E., Barlow, M., and Hoell, A.: Warming of the Indian Ocean threatens eastern and southern African food security but could be mitigated by agricultural development, *P. Natl. Acad. Sci. USA*, 105, 11081–11086, 2008.
- Funk, C., Michaelsen, J., and Marshall, M.: Mapping recent decadal climate variations in precipitation and temperature across Eastern Africa and the Sahel, in: *Remote Sensing of Drought: Innovative Monitoring Approaches*, edited by: Wardlow, B., Anderson, M., and Verdin, J., CRC Press, Boca Raton, Florida, USA, 25 pp., 2012.
- Funk, C., Husak, G., Michaelsen, J., Shukla, S., Hoell, A., Lyon, B., Hoerling, M. P., Liebmann, B., Zhang, T., Verdin, J., Galu, G., Eilerts, G., and Rowland, J.: Attribution of 2012 and 2003–12 rainfall deficits in eastern Kenya and southern Somalia, *B. Am. Meteorol. Soc.*, 94, 45–48, 2013.

## Predicting East African spring droughts

C. Funk et al.

Title Page

Abstract

Introduction

Conclusions

References

Tables

Figures

◀

▶

◀

▶

Back

Close

Full Screen / Esc

Printer-friendly Version

Interactive Discussion



## Predicting East African spring droughts

C. Funk et al.

Title Page

Abstract

Introduction

Conclusions

References

Tables

Figures

◀

▶

◀

▶

Back

Close

Full Screen / Esc

Printer-friendly Version

Interactive Discussion



Funk, C., Peterson, P., Landsfeld, M., Pedreros, D., Verdin, J., Rowland, J., Romero, B., Husak, G., Michaelsen, J., and Verdin, A.: A Quasi-global Precipitation Time Series for Drought Monitoring, USGS, EROS Data Center, Sioux Falls, SD, USA, 2014.

Gill, A. E.: Some simple solutions for heat-induced tropical circulation, *Q. J. Roy. Meteorol. Soc.*, 106, 447–462, 1980.

Hastenrath, S., Polzin, D., and Mutai, C.: Circulation mechanisms of Kenya rainfall anomalies, *J. Climate*, 24, 404–412, 2011.

Hoell, A. and Funk, C.: The ENSO-related west pacific sea surface temperature gradient, *J. Climate*, 26, 9545–9562, doi:10.1175/JCLI-D-12-00344.1, 2013a.

Hoell, A. and Funk, C.: Indo-Pacific sea surface temperature influences on failed consecutive rainy seasons over Eastern Africa, *Clim. Dynam.*, doi:10.1007/s00382-013-1991-6, in press, 2013b.

Hoell, A. and Funk, C.: The forcing of March–May East Africa rainfall by the warming trend in Pacific sea surface temperatures and Pacific Decadal Variability, *Clim. Dynam.*, doi:10.1007/s00382-013-1991-6, in press, 2013c.

Hoell, A., Funk, C., and Barlow, M.: The regional forcing of Northern Hemisphere drought during recent warm tropical west Pacific Ocean La Niña events, *Clim. Dynam.*, doi:10.1007/s00382-013-1799-4, in press, 2013.

Hoell, A., Funk, C., and Barlow, M.: La Nina diversity and the forcing of Northwest Indian Ocean rim teleconnections, *Clim. Dynam.*, in press, 2014.

Jury, M. R.: Ethiopian decadal climate variability, *Theor. Appl. Climatol.*, 101, 29–40, 2010.

Jury, M. R. and Funk, C.: Climatic trends over Ethiopia: regional signals and drivers, *Int. J. Climatol.*, 33, 1924–1935, doi:10.1002/joc.3560, 2013.

Liebmann, B., Bladé, I., Kiladis, G. N., Carvalho, L. M., B. Senay, G., Allured, D., Leroux, S., and Funk, C.: Seasonality of African precipitation from 1996 to 2009, *J. Climate*, 25, 4304–4322, 2012.

Liebmann, B., Hoerling, M. P., Funk, C., Bladé, I., Dole, R. M., Allured, D., Pegion, P., and Eischeid, J. K.: Understanding Eastern Horn of Africa rainfall variability and change, *J. Climate*, in review, 2013.

Lyon, B. and DeWitt, D. G.: A recent and abrupt decline in the East African long rains, *Geophys. Res. Lett.*, 39, L02702, doi:10.1029/2011gl050337, 2012.

## Predicting East African spring droughts

C. Funk et al.

[Title Page](#)

[Abstract](#)

[Introduction](#)

[Conclusions](#)

[References](#)

[Tables](#)

[Figures](#)

[⏪](#)

[⏩](#)

[◀](#)

[▶](#)

[Back](#)

[Close](#)

[Full Screen / Esc](#)

[Printer-friendly Version](#)

[Interactive Discussion](#)



Lyon, B., Barnston, A. G., and DeWitt, D. G.: Tropical pacific forcing of a 1998–1999 climate shift: observational analysis and climate model results for the boreal spring season, *Clim. Dynam.*, doi:10.1007/s00382-013-1891-9, in press, 2013.

5 McKee, T. B., Doesken, N. J., and Kleist, J.: The relationship of drought frequency and duration to time scales, *Proceedings of the 8th Conference on Applied Climatology*, 17–22 January 1993, Anaheim, California, 179–183, 1993.

Mwangi, E., Wetterhall, F., Dutra, E., Di Giuseppe, F., and Pappenberger, F.: Forecasting droughts in East Africa, *Hydrol. Earth Syst. Sci.*, 18, 611–620, doi:10.5194/hess-18-611-2014, 2014.

10 Pohl, B. and Camberlin, P.: Influence of the Madden–Julian Oscillation on East African rainfall, I: Intraseasonal variability and regional dependency, *Q. J. Roy. Meteorol. Soc.*, 132, 2521–2539, 2006.

Saji, N. H., Goswami, B. N., Vinayachandran, P. N., and Yamagata, T.: A dipole mode in the tropical Indian Ocean, *Nature*, 401, 360–363, 1999.

15 Schneider, U., Becker, A., Finger, P., Meyer-Christoffer, A., Ziese, M., and Rudolf, B.: GPCP's new land surface precipitation climatology based on quality-controlled in situ data and its role in quantifying the global water cycle, *Theor. Appl. Climatol.*, 115, 1–26, doi:10.1007/s00704-013-0860-x, 2013.

20 Sheffield, J., Wood, E. F., Chaney, N., Guan, K., Sadri, S., Yuan, X., Olang, L., Amani, A., Ali, A., and Demuth, S.: A drought monitoring and forecasting system for sub-Saharan African water resources and food security, *B. Am. Meteorol. Soc.*, doi:10.1175/BAMS-D-12-00124.1, in press, 2013.

Shukla, S., Sheffield, J., Wood, E. F., and Lettenmaier, D. P.: On the sources of global land surface hydrologic predictability, *Hydrol. Earth Syst. Sci.*, 17, 2781–2796, doi:10.5194/hess-17-2781-2013, 2013.

25 Shukla, S., Mcnally, A. P., Husak, G., and Funk, C.: Seasonal hydrologic forecast system for food insecure regions of East Africa, *Hydrol. Earth Syst. Sci. Discuss.*, submitted, 2014.

Smith, T. M., Reynolds, R. W., Peterson, T. C., and Lawrimore, J.: Improvements to NOAA's historical merged land–ocean surface temperature analysis (1880–2006), *J. Climate*, 21, 2283–2296, doi:10.1175/2007jcli2100.1, 2008.

30 Taylor, K. E., Stouffer, R. J., and Meehl, G. A.: An overview of CMIP5 and the experiment design, *B. Am. Meteorol. Soc.*, 93, 485–498, doi:10.1175/bams-d-11-00094.1, 2011.

Tierney, J., Smerdon, J., Anchukaitis, K., and Seager, R.: Multidecadal variability in East African hydroclimate controlled by the Indian Ocean Peer reviewed article, *Nature*, 493, 389–392, 2013.

Verdin, J., Funk, C., Senay, G., and Choularton, R.: Climate science and famine early warning, *Philos. T. Roy. Soc. B*, 360, 2155–2168, 2005.

Ververs, M.-T.: The east African food crisis: did regional early warning systems function?, *J. Nutr.*, 142, 131–133, doi:10.3945/jn.111.150342, 2011.

Viste, E., Korecha, D., and Sorteberg, A.: Recent drought and precipitation tendencies in Ethiopia, *Theor. Appl. Climatol.*, 112, 1–17, 2012.

Williams, A. and Funk, C.: A westward Extension of the tropical Pacific warm pool leads to leads to March through June drying in Kenya and Ethiopia, Sioux Falls, SD, USA, 2010.

Williams, A., Funk, C., Michaelsen, J., Rauscher, S., Robertson, I., Wils, T., Koprowski, M., Eshetu, Z., and Loader, N.: Recent summer precipitation trends in the Greater Horn of Africa and the emerging role of Indian Ocean sea surface temperature, *Clim. Dynam.*, 39, 2307–2328, doi:10.1007/s00382-011-1222-y, 2011.

Williams, P. and Funk, C.: A westward extension of the warm pool leads to a westward extension of the Walker circulation, drying eastern Africa, *Clim. Dynam.*, 37, 2417–2435, doi:10.1007/s00382-010-0984-y, 2011.

## HESSD

11, 3111–3136, 2014

### Predicting East African spring droughts

C. Funk et al.

Title Page

Abstract

Introduction

Conclusions

References

Tables

Figures

⏪

⏩

◀

▶

Back

Close

Full Screen / Esc

Printer-friendly Version

Interactive Discussion



## Predicting East African spring droughts

C. Funk et al.

Title Page

Abstract

Introduction

Conclusions

References

Tables

Figures

◀

▶

◀

▶

Back

Close

Full Screen / Esc

Printer-friendly Version

Interactive Discussion



**Table 1.** Coupled ocean–atmosphere models used in this study.

|   |
|---|
| Modeling Group  |
| Commonwealth Scientific and Industrial Research Organization (CSIRO) and Bureau of Meteorology (BOM), Australia   |
| Canadian Centre for Climate Modelling and Analysis  |
| National Center for Atmospheric Research  |
| Community Earth System Model Contributors   |
| Centre National de Recherches Météorologiques/Centre Européen de Recherche et Formation Avancée en Calcul Scientifique  |
| EC-EARTH consortium   |
| The First Institute of Oceanography, SOA, China   |
| NOAA Geophysical Fluid Dynamics Laboratory  |
| NASA Goddard Institute for Space Studies  |
| Met Office Hadley Centre  |
| Institute for Numerical Mathematics   |
| Institut Pierre-Simon Laplace   |
| Atmosphere and Ocean Research Institute (The University of Tokyo), National Institute for Environmental Studies, and Japan Agency for Marine–Earth Science and Technology |
| Max-Planck-Institut für Meteorologie (Max Planck Institute for Meteorology)   |

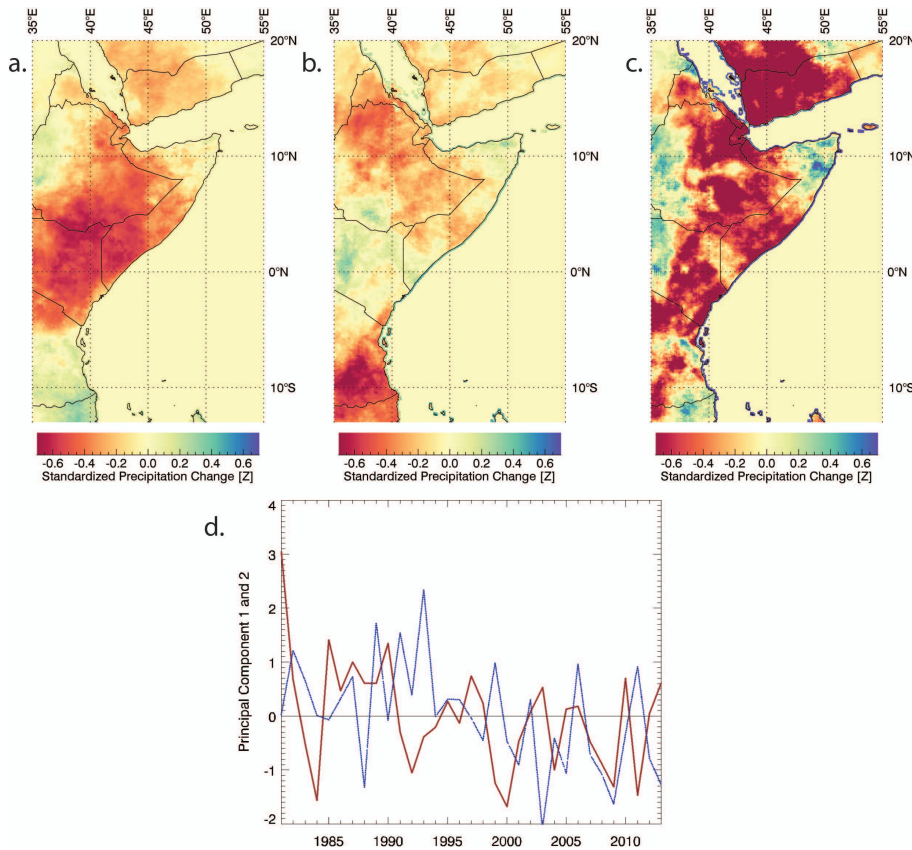


**Fig. 1.** (a) Twenty year changes in standardized March–May precipitation associated with the trend in principal component 1. (b) same for principal component 2. (c) Twenty year changes in standardized March–May precipitation associated with a linear trend. (d) Standardized time series of PC1 (solid red line) and PC2 (dashed blue line).

## Predicting East African spring droughts

C. Funk et al.

Title Page

Abstract

Introduction

Conclusions

References

Tables

Figures

◀

▶

◀

▶

Back

Close

Full Screen / Esc

Printer-friendly Version

Interactive Discussion



## Predicting East African spring droughts

C. Funk et al.

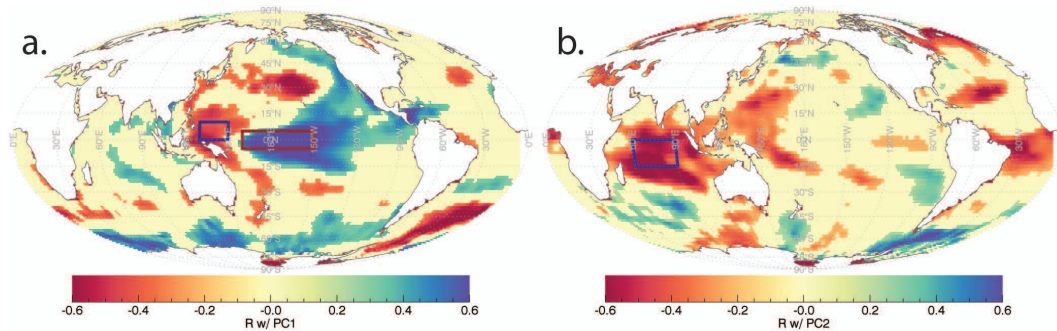


**Fig. 2.** (a) Correlations between March–May CHIRPS PC1 and January SSTs. (b) same for CHIRPS PC2. Values have been screened at a 10 % significance level. Boxes in panel a and b show the regions used to define the WPG and CIO SST indices.

[Title Page](#)[Abstract](#)[Introduction](#)[Conclusions](#)[References](#)[Tables](#)[Figures](#)[◀](#)[▶](#)[◀](#)[▶](#)[Back](#)[Close](#)[Full Screen / Esc](#)[Printer-friendly Version](#)[Interactive Discussion](#)

## Predicting East African spring droughts

C. Funk et al.

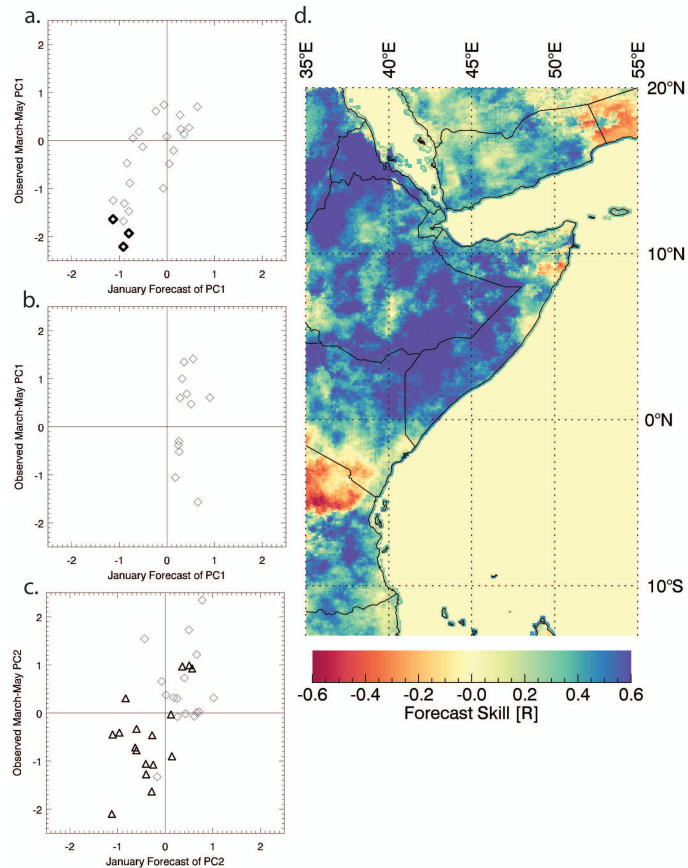


**Fig. 3.** (a) Scatterplot of 1994–2013 March–May PC1 observations ( $y$  axis) and PC1 estimates based on January WPG SSTs ( $x$  axis). (b) Same but for 1981–1993. (c) Scatterplot of 1981–2013 March–May PC2 observations ( $y$  axis) and PC1 estimates based on January WPG SSTs ( $x$  axis). (d) 1993–2013 correlation between forecasts and observed rainfall.

[Title Page](#)
[Abstract](#)
[Introduction](#)
[Conclusions](#)
[References](#)
[Tables](#)
[Figures](#)
[⏪](#)
[⏩](#)
[◀](#)
[▶](#)
[Back](#)
[Close](#)
[Full Screen / Esc](#)
[Printer-friendly Version](#)
[Interactive Discussion](#)


## Predicting East African spring droughts

C. Funk et al.

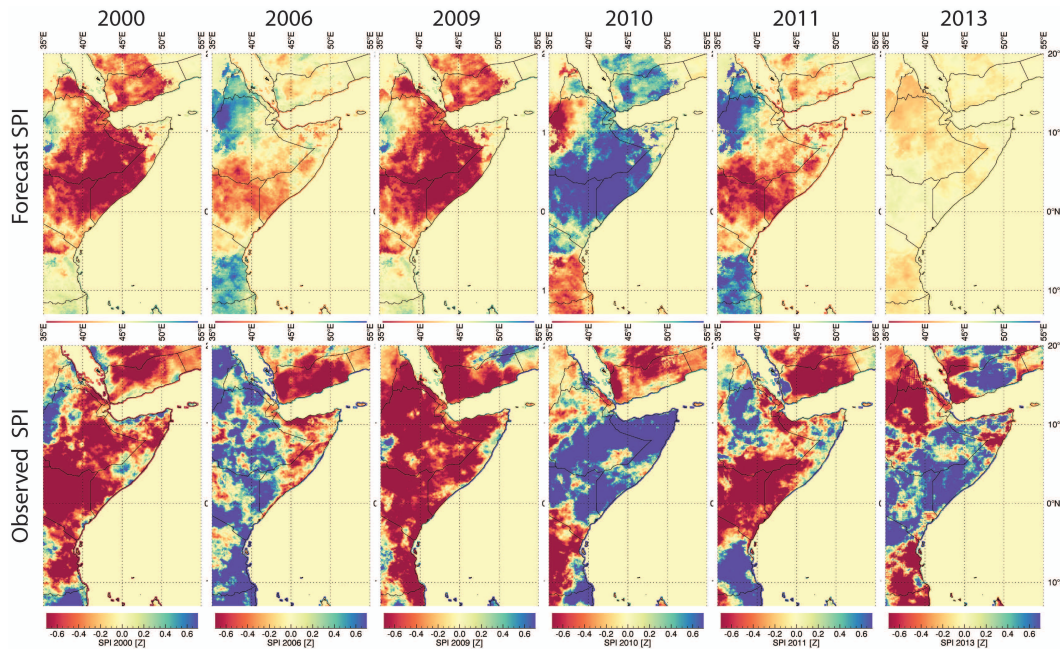


**Fig. 4.** Forecasts and observed March–May SPI values for 2000, 2006, 2009, 2010, 2011 and 2013.

[Title Page](#)[Abstract](#)[Introduction](#)[Conclusions](#)[References](#)[Tables](#)[Figures](#)[⏪](#)[⏩](#)[⏴](#)[⏵](#)[Back](#)[Close](#)[Full Screen / Esc](#)[Printer-friendly Version](#)[Interactive Discussion](#)

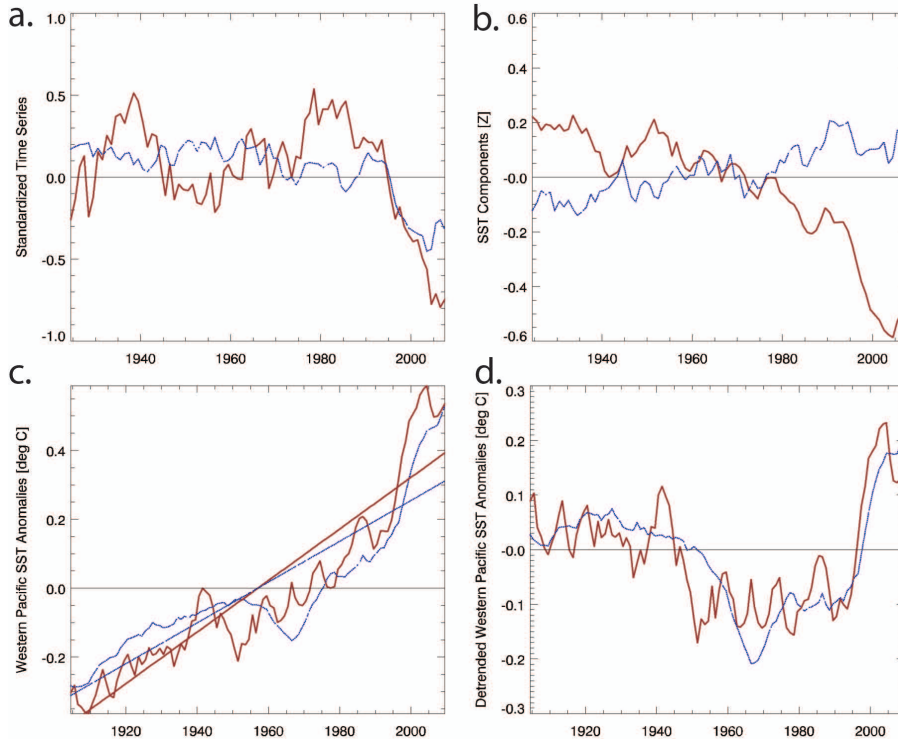


**Fig. 5.** (a) Time series of smoothed standardized GPCC for study region (red solid line), and WPG-based estimates of GPCC SPI (blue dashed line) and Niño 4 (dashed blue line) contributions to the GPCC estimates shown in blue in (a). (c) Observed western Pacific SST anomalies (solid red line), CMIP5 western Pacific SST anomalies (dashed blue line), and linear fits (straight red and blue lines). (d) Detrended western Pacific SST anomalies (solid red line) and detrended CMIP5 western Pacific SST anomalies (dashed blue line).

**Predicting East African spring droughts**

C. Funk et al.

Title Page

Abstract

Introduction

Conclusions

References

Tables

Figures

◀

▶

◀

▶

Back

Close

Full Screen / Esc

Printer-friendly Version

Interactive Discussion

